miR-380-5p represses p53 to control cellular survival and is associated with poor outcome in *MYCN*-amplified neuroblastoma

Alexander Swarbrick[1,2,20], Susan L Woods[3,4,20], Alexander Shaw[1,5,6], Asha Balakrishnan[7], Yuwei Phua[1,2], Akira Nguyen[1], Yvan Chanthery[8], Lionel Lim[8], Lesley J Ashton[9], Robert L Judson[8], Noelle Huskey[8], Robert Blelloch[10,11], Michelle Haber[9], Murray D Norris[9], Peter Lengyel[7], Christopher S Hackett[8], Thomas Preiss[2,5,6], Albert Chetcuti[12], Christopher S Sullivan[13], Eric G Marcusson[14], William Weiss[15,16], Noelle L'Etoile[17] & Andrei Goga[7,18,19]

Inactivation of the p53 tumor suppressor pathway allows cell survival in times of stress and occurs in many human cancers; however, normal embryonic stem cells and some cancers such as neuroblastoma maintain wild-type human *TP53* and mouse *Trp53* (referred to collectively as *p53* herein). Here we describe a miRNA, miR-380-5p, that represses p53 expression via a conserved sequence in the *p53* 3′ untranslated region (UTR). miR-380-5p is highly expressed in mouse embryonic stem cells and neuroblastomas, and high expression correlates with poor outcome in neuroblastomas with neuroblastoma derived v-myc myelocytomatosis viral-related oncogene (*MYCN*) amplification. miR-380 overexpression cooperates with activated HRAS oncoprotein to transform primary cells, block oncogene-induced senescence and form tumors in mice. Conversely, inhibition of endogenous miR-380-5p in embryonic stem or neuroblastoma cells results in induction of p53, and extensive apoptotic cell death. *In vivo* delivery of a miR-380-5p antagonist decreases tumor size in an orthotopic mouse model of neuroblastoma. We demonstrate a new mechanism of p53 regulation in cancer and stem cells and uncover a potential therapeutic target for neuroblastoma.

The p53 tumor suppressor is activated after a wide variety of genotoxic stresses, resulting in cell cycle arrest, apoptosis or senescence[1,2]. Inactivation of p53 is a common event in cancer[3,4] and attempts to reactivate p53 function are being vigorously pursued as cancer therapeutics[5–8]. However, in some cancers, including more than 99% of primary neuroblastomas, *TP53* remains wild type[9]. After treatment with chemotherapy, alterations in p53 pathway components are frequently found to occur in neuroblastomas[9]. This suggests that complete inactivation of the p53 pathway is required for tumor cells to survive chemotherapy. How wild-type p53 can be tolerated by neuroblastoma cells before treatment is unclear, suggesting that other mechanisms exist to attenuate p53 function.
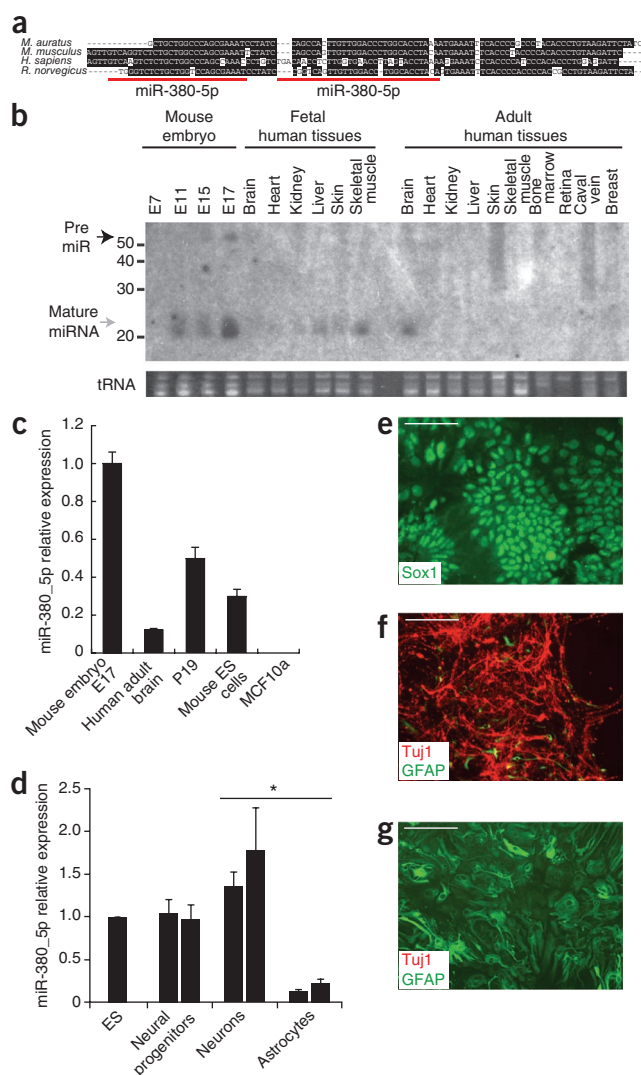
Changes in the abundance of p53 can modulate p53-mediated transcription[10,11] and the resulting biological outputs, such as apoptosis[12–14]. Even modest decreases in p53 abundance can lead to greatly reduced activation of a p53 reporter gene *in vivo*[15]. Notably, 50% of the tumors that form in *Trp53*^{+/−} mice retain the wild-type *Trp53* allele[16], suggesting that a modest reduction in wild-type p53 promotes tumorigenesis.

The *TP53* mRNA has a complex 3′ UTR, and highly conserved sequences within the 3′ UTR control *TP53* translation through poorly understood mechanisms[17]. MiRNAs are small noncoding RNAs that control gene expression by regulating mRNA translation, stability or both, typically by binding regions of homology in the 3′ UTR of target mRNAs[18]. Several miRNAs with validated roles in the promotion or suppression of neoplasia have been identified[19,20].

Here we show that p53 is regulated in human cancer by miR-380-5p. We find that this miRNA is highly expressed in the majority of primary

Figure 1 The *p53* 3′ UTR contains binding sites for miR-380-5p, a developmentally restricted miRNA. (**a**) Alignment of human, mouse, rat and hamster *p53* 3′ UTRs, identifying a highly conserved 104-bp region. The predicted miR-380-5p binding sites are indicated in red. (**b**) Northern blot of miR-380 using total RNA from mouse embryonic, human fetal and adult tissues. (**c**) Quantitative RT-PCR (qRT-PCR) analysis of miR-380-5p expression in normal brain, embryonic carcinoma (P19) and mouse ES cells. (**d**) qRT-PCR analysis showing miR-380-5p expression in ES cells differentiated to the neuronal lineage. (**e**) Immunofluorescent staining for Sox1 (green) in cultures of neural progenitor cells. Scale bar, 65 μm. (**f**,**g**) Immunofluorescent staining for an early neuronal marker, Tuj1 (red), and a marker of astrocytes, GFAP (green), in differentiated cultures of neurons (**f**) and astrocytes (**g**). Scale bars: 150 μm (**f**); 100 μm (**g**). In **c** and **d**, error bars depict s.d.; in **d**, independent biological replicates indicated by separate bars. *$P < 0.0002$.

of both putative binding sites featured a preponderance of adjacent destabilizing structures (loops, single-stranded regions and free ends) and only short stem structures, features preferred for miRNA–3′ UTR interactions (**Supplementary Table 1**).

miR-380-5p is encoded within a large miRNA cluster found in an imprinted region of human 14q32 (ref. 25). We detected abundant miR-380 expression in mouse embryonic tissue, human fetal tissue and adult human brain (**Fig. 1b**), tissues in which p53 has key roles[26], but not in other adult tissues. miR-380-5p was also highly expressed in mouse ES cells and P19 embryonic carcinoma cells, as determined by quantitative RT-PCR (**Fig. 1c**). Human breast MCF10A cells do not express detectable miR-380-5p, and we used them as a negative control line (**Fig. 1c**). MiR-380-5p expression was maintained in mouse ES cells differentiated in culture to Sox1^{+} neural progenitors and Tuj1^{+} neurons, but not in cultures containing predominantly Gfap[+] astrocytes (**Fig. 1d–g**). Thus, miR-380-5p is not simply a marker of undifferentiated cells but is also expressed through neuronal specification.

miR-380-5p suppresses p53 and apoptosis in stem cells

To examine the function of endogenous miR-380-5p, we used a locked nucleic acid (LNA)-modified antisense oligomer to inhibit miR-380-5p (LNA-380). Transfection of LNA-380, but not a control LNA, partially relieved repression of a luciferase reporter with three perfect miR-380-5p binding sites in the 3′ UTR (**Fig. 2a**). Activity of a control reporter after transfection of miR-380-5p alone or with control LNA or LNA-380 was not changed (data not shown). Transfection of mouse ES cells with LNA-380 resulted in changes in ES cell morphology, diminished colony size, an increased number of nonadherent cells after 8 h (data not shown), and substantial cell death 24 h after treatment (**Fig. 2b**). Although *Trp53*^{−/−} ES cells express similar levels of miR-380-5p to their wild-type counterparts, LNA-380 treatment of *Trp53*^{−/−} ES cells did not induce cell death (**Fig. 2b,c**), demonstrating a requirement for p53 in cell death induced by LNA-380. Inhibition of miR-380-5p was accompanied by the upregulation of p53 protein and the apoptotic marker cleaved poly(ADP)-ribose polymerase (PARP) (**Fig. 2d**) in wild-type ES cells but not *Trp53*^{−/−} cells. We observed this effect over a range of LNA-380 concentrations but not in wild-type ES cells treated with a variety of scrambled and other control LNAs (**Supplementary Fig. 1a–c**). As an additional control, we tested whether mature miRNAs are required for induction of p53 expression by LNA-380. ES cells that are deficient in mature miRNA species (including miR-380-5p, **Fig. 2c**) owing to homologous deletion of DiGeorge syndrome critical region-8 (*Dgcr8*), remain responsive to genotoxic shock, and p53 expression is induced after ultraviolet irradiation (**Fig. 2d**). However, treatment of *Dgcr8*^{−/−} ES

neuroblastomas and functions as a proto-oncogene in a mouse mammary transplant model. miR-380-5p is predicted to bind to a highly conserved region in the *TP53* 3′ UTR. Inhibition of miR-380-5p results in upregulation of p53 in embryonic stem (ES) and neuroblastoma cells and the induction of apoptosis, as well as diminished tumor growth *in vivo*. Our results identify a new therapeutic approach to reactivate p53 in neuroblastoma.

RESULTS
The *TP53* 3′UTR has two potential binding sites for miR-380-5p
We identified a 104-bp region of high homology in the *p53* 3′ UTR shared across human, mouse, rat and hamster species but not conserved in nonmammalian species (**Fig. 1a**). This corresponds to nucleotides (582–685) of the human *TP53* 3′ UTR. Human and mouse *TP53* and *Trp53* 3′ UTRs share 78% identity within this region. This is similar to the 84% identity found when comparing the coding portion of human *TP53* exon 11 with the corresponding sequence from mouse, suggesting that this region of the 3′ UTR may have functional importance. With the miRanda algorithm[21] we identified two predicted adjacent target sites for miR-380-5p within the conserved 3′ UTR region (**Fig. 1a**) at a spacing previously reported to enhance cooperative repression[22]. Local RNA structure is proposed to regulate the efficiency of miRNA binding to target UTRs[23,24]. The sequence
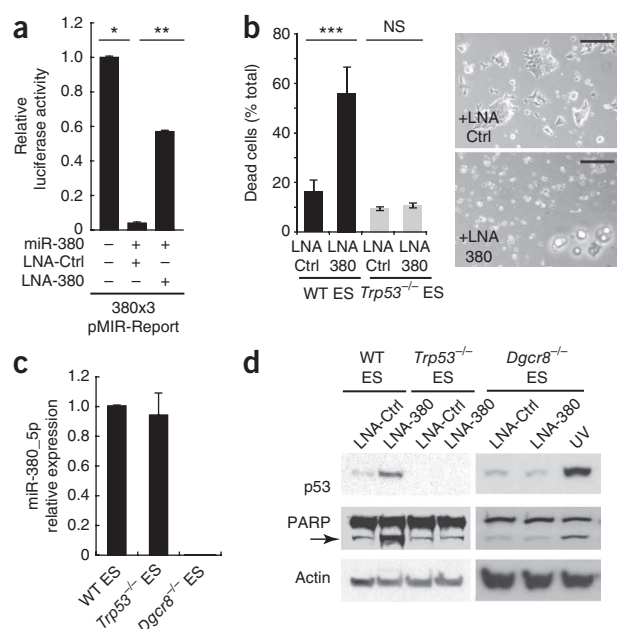
Figure 2 miR-380-5p is required for ES cell survival. (**a**) Activity of a miR-380 reporter either alone or after transfection with a control LNA (LNA-Ctrl) or an LNA directed against miR-380-5p (LNA-380). (**b**) Left, amount of ES cell death 24h after transfection of wild-type (WT) or *Trp53*$^{-/-}$ ES cells with LNA-Ctrl or LNA-380. Right, cell images 24 h post transfection with LNA-Ctrl or LNA-380. (**c**) qRT-PCR analysis of relative miR-380-5p expression in WT, *Trp53*$^{-/-}$ and *Dgcr8*$^{-/-}$ ES cells. (**d**) Western blots showing p53 induction and PARP cleavage (indicated by the arrow) after knockdown of miR-380-5p by LNA-380 compared to LNA-ctrl–transfected wild-type, *Trp53*$^{-/-}$ and *Dgcr8*$^{-/-}$ ES cells that were ultraviolet irradiated (UV). In **a**, **b** and **d**, results are from at least three independent experiments (performed in triplicate in **c**). In **a**–**c**, error bars depict s.d. *$P < 0.00002$; **$P < 0.00007$; ***$P < 0.0004$; NS, not significant. Scale bars, 200 µm.

the transcriptional control and regulation of mature miR-380-5p stability, this suggests that ES cells have an built-in mechanism to minimize miR-380-5p levels in situations of cellular stress.

Ectopic expression of miR-380 is sufficient to suppress p53

We transfected human MCF10A cells, which express wild-type p53 but not detectable miR-380-5p, with miR-380-5p or a nontargeting control miRNA mimic (**Supplementary Fig. 2a**). Expression of miR-380-5p resulted in a significant ~40% decrease in basal p53 protein levels (**Fig. 3a,b**). UV irradiation led to a dose-dependent increase in p53 protein expression that was suppressed by the expression of miR-380-5p (**Fig. 3a,b**). There was no significant difference in *TP53* mRNA levels after miR-380-5p overexpression (**Fig. 3c**), suggesting a predominant role for the miRNA in the regulation of *TP53* translation rather than mRNA stability. For comparison, we transfected cells with miR-125b, which has recently been suggested to target p53 (ref. 27), but we did not detect a significant effect of miR-125b on either *TP53* mRNA or protein levels (**Supplementary Fig. 2b,c**). We obtained similar results with MCF7 and MCF10A cell lines that stably express miR-380 or a scrambled miRNA control (**Supplementary Fig. 2d–g**). Together with our data from ES cells (**Fig. 2** and **Supplementary Fig. 1**), these results suggest that miR-380-5p acts to directly regulate p53 translation rather than the stability of the mRNA or protein.

We next asked whether miR-380 expression directly regulates p53 protein expression via the conserved 104-bp element within the *TP53* 3′ UTR predicted to encode the two miR-380-5p binding sites (**Fig. 1a**).

cells with LNA-380 did not induce p53 expression (**Fig. 2d**). Together, these data show that inhibition of endogenous miR-380-5p in ES cells results in upregulation of p53 and apoptotic cell death. At just 4 h after transfection of ES cells with LNA-380, cell morphology is indistinguishable from control LNA-treated cells (data not shown); however, p53 abundance is already increased (**Supplementary Fig. 1d**). This increase in p53 protein is not due to stabilization of the protein, as the half-life of p53 is unchanged in LNA-380–treated cells compared to LNA-control–treated cells (**Supplementary Fig. 1e**). In contrast, 4 h after ultraviolet irradiation, p53 protein was robustly stabilized (**Supplementary Fig. 1e**). Amounts of the p53 regulators p19^{ARF}, Mdm2 and Chek2 were unchanged by LNA-380 treatment (**Supplementary Fig. 1f**).
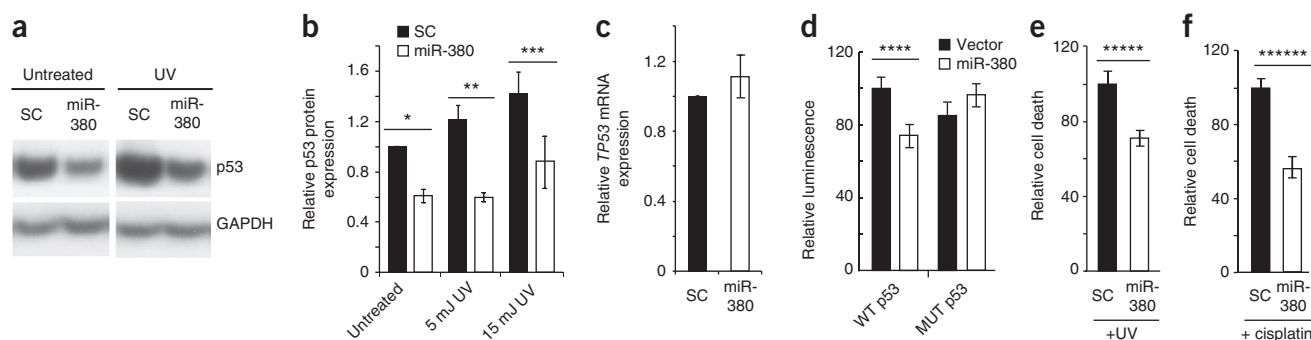
Treatment of ES cells with ultraviolet radiation leads to the rapid accumulation of p53 (**Supplementary Fig. 1g**). Of note, endogenous expression of miR-380-5p but not another miRNA from the same genomic cluster (miR-323) or an unrelated miRNA (miR-16) decreased in a manner inversely correlated with p53 protein expression (**Supplementary Fig. 1g**). Although little is known about

Figure 3 miR-380-5p targets p53 and decreases cell death after genotoxic stress. (**a**) Western blot showing p53 expression in MCF10a cells transfected with either a scrambled (SC) miRNA or miR-380-5p. (**b**) Quantification of p53 protein in MCF10a cells transfected with SC miRNA or miR-380-5p with or without UV treatment, normalized to glyceraldehyde-3-phosphate dehydrogenase (GAPDH). (**c**) qRT-PCR analysis of *TP53* mRNA in MCF10a cells after expression of miR-380, normalized to *GAPDH* levels. (**d**) Luciferase activity of *TP53* 3′UTR reporters after expression of miR-380. (**e,f**) Relative cell death of MCF10a cell populations stably expressing miR-380 or SC 24 h after treatment with ultraviolet light (**e**) or cisplatin (**f**). Error bars depict s.e.m. (**b,c**) or s.d. (**d–f**). **a,b** and **d–f** are results from at least three independent repeats; In **c** experiments were performed in triplicate. *$P < 0.0009$, **$P < 0.03$, ***$P < 0.002$, ****$P < 0.05$, *****$P < 0.03$, ******$P < 0.001$.

We generated a luciferase reporter construct that contains a single 104-bp wild-type human *TP53* element downstream of the luciferase open reading frame (WT-p53) or a reporter construct in which the nucleotides complementary to the miR-380-5p seed sequences were deleted (MUT-p53). These reporter constructs lack the remainder of the *TP53* 3′ UTR that contains other previously identified translational regulatory elements[28,29]. When the WT-p53 reporter was transfected along with miR-380 into human embryonic kidney cells, luciferase activity was decreased ~30% compared to cells transfected with a control vector (**Fig. 3d**). Suppression of luciferase activity was not observed when the MUT-p53 reporter was transfected with miR-380 (**Fig. 3d**). Thus, miR-380-5p can directly attenuate translation via elements found in the *TP53* 3′ UTR.

We next asked whether miR-380 overexpression can regulate apoptosis. Twenty-four hours after treatment with two different DNA damaging agents, ultraviolet light or cisplatin, we observed significantly more cell death in control cells than in those expressing miR-380 (**Fig. 3e,f**). We saw no appreciable cell death in the absence of ultraviolet light or cisplatin treatment (data not shown).

## miR-380 blocks senescence and acts as an oncogene *in vivo*

A stringent test of oncogene function in cancer is the ability to induce tumor formation *de novo* in mouse models. Loss of p53 function cooperates with activated HRAS expression to induce a variety of tumors, including mammary cancers[30,31]. We tested whether expression of miR-380 can similarly cooperate with activated HRAS to transform primary mouse mammary epithelial cells (MMECs). The unique biology of the mammary gland enabled us to use a transplantation technique that rapidly generates transgenic mammary glands *in vivo*[32] and can be used as an *in vivo* model of cellular transformation in a system with an intact p53 pathway. MMECs from naive FVB/N mice were collected and cultured for 72 h, during which time the cells were infected with a retrovirus encoding activated *HRAS* and retrovirus encoding various small RNAs. Cells were subsequently transplanted into the cleared mammary fat pad of syngeneic mice (**Supplementary Fig. 3a**). Expression of activated HRAS with either miR-380 or a small hairpin RNA that specifically targets mouse *Trp53*[33] (shRNA p53) resulted in downregulation of a key transcriptional target of p53, Cdkn1a (also known as p21[waf1]); in contrast to cells expressing activated HRAS and a scrambled control miRNA (**Supplementary Fig. 3b**). Mice receiving MMECs expressing activated HRAS plus a control retrovirus infrequently developed small tumors (**Fig. 4a**). In contrast, expression of activated HRAS with either miR-380 or shRNA p53 resulted in a substantially greater frequency of tumor formation (**Fig. 4a**). We saw no significant

differences in tumor latency or growth rates between the shRNA p53 and miR-380 groups (**Supplementary Fig. 3c**). Expression of miR-125b with activated HRAS resulted in even fewer tumors than in the control mice (**Fig. 4a**), consistent with a role for miR-125b in attenuating the proliferation of breast epithelium[34]. We observed elevated levels of miR-380-5p expression in all tumors tested (**Fig. 4b**), and the average expression across these tumors was within the physiological range of expression observed in primary neuroblastomas (**Supplementary Fig. 4a**).

Tumors expressing activated HRAS plus control viral constructs were cystic in nature and mostly comprised inflammatory cell infiltrates (**Fig. 4c**). In contrast, miR-380 or shRNA p53 expression together with activated HRAS resulted in solid rather than cystic tumors that were comprised predominantly of epithelial cells (**Fig. 4c**). Activated HRAS has been shown to induce senescence in a variety of tumor models in a p53-dependent manner[8,30]. Tumor cells expressing activated HRAS plus control (empty vector or scrambled control) stained positive for senescence-associated β-galactosidase (**Fig. 4c**). In contrast, tumors expressing HRAS plus miR-380 or shRNA p53 did not express senescence markers (**Fig. 4c**). p21[waf1] expression was higher in wild-type mouse mammary epithelial cells and tumor cells expressing activated HRAS plus control viral constructs, than in tumor cells that expressed HRAS and miR-380 or shRNA p53 (**Fig. 4c,d**). These data are consistent with a role for miR-380 in promoting mammary tumorigenesis by suppressing the p53- and p21[waf1]-dependent oncogene-induced senescence program initiated by activated HRAS.

miR-380-5p and outcome in *MYCN*-amplified neuroblastoma

Virtually all neuroblastomas have wild-type *TP53* before treatment with chemotherapy, suggesting that the p53 pathway may be attenuated
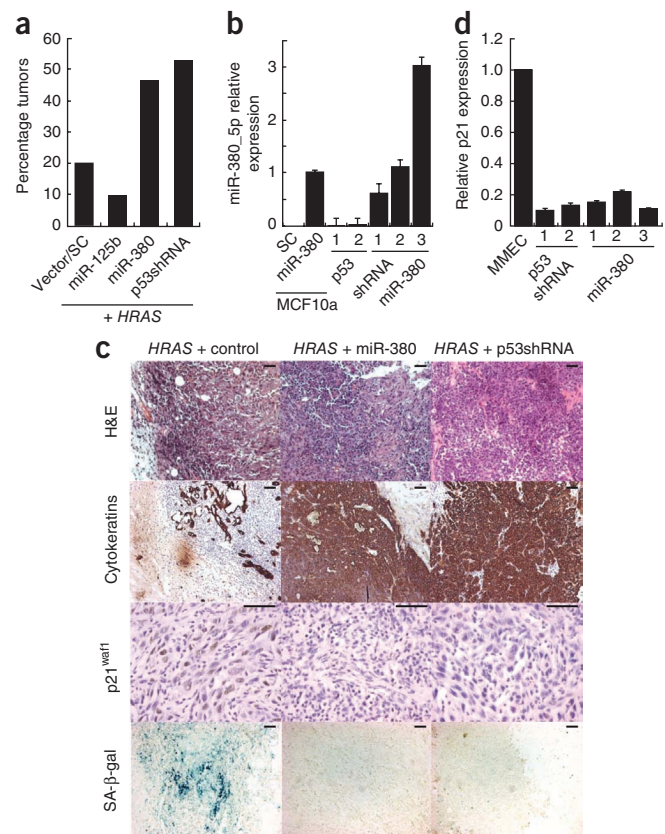

Figure 4 miR-380 prevents oncogene-induced senescence and increases tumor incidence in a mouse mammary cancer model. (**a**) The incidence of palpable mammary tumors (1 tumor per mouse) arising from cells infected with the indicated miRNA-encoding retrovirus plus *HRAS*[V12] after 6 weeks, control group with empty vector or expressing scrambled control (vector/SC). $n = 15$; miR-125b, $n = 10$; miR-380, $n = 15$; p53 shRNA, $n = 17$. (**b**) qRT-PCR of mature miR-380-5p in tumors arising from cells infected with *HRAS*[V12] and miR-380 or p53 shRNA virus. MCF10a cells that stably express miR-380 or a scrambled miRNA are shown as controls. (**c**) Immunohistochemical staining of mammary tumors. SA-β-gal, senescence-associated β-galactosidase. (**d**) qRT-PCR for *p21*[waf1] expression normalized to *GAPDH* in tumors arising from cells infected with *HRAS*[V12] and p53 shRNA or miR-380 retrovirus compared to the primary MMECs. In **b** and **d**, error bars depict s.d.; each column represents a separate tumor. Scale bars, 100 μm.

Figure 5 miR-380-5p is expressed in mouse and human neuroblastoma and is associated with poor outcome in subjects with *MYCN* amplification. (**a**) qRT-PCR for miR-380-5p expression in tumors and neuroendocrine ganglion (SCG) tissue from wild type and transgenic mice. (**b**) miR-380-5p expression detected by qRT-PCR in primary human neuroblastoma samples taken before chemotherapy. miR-380-5p expression was normalized to U6 small nuclear 2 RNA, normal human brain expression (indicated by red dashed line); 'low' and 'high' designate the lowest quartile of miR-380-5p expression and the remainder, respectively. (**c**) Kaplan-Meier survival curves of event-free survival (EFS) in subgroups of subjects with neuroblastoma according to relative expression level of miR-380-5p, all with *MYCN* amplification (*n* = 22). Subjects were dichotomized around the lower quartile of miR-380-5p expression. High: *n* = 6, mean miR-380-5p expression = 3.19, s.e.m. = 0.83. Low: *n* = 16, mean miR-380-5p expression = 0.49, s.e.m. = 0.13. *P* = 0.004. In **a**, error bars depict s.d., *$P < 0.02$, **$P < 0.02$.

by another mechanism in these tumors[35]. We examined miR-380-5p and p53 expression in neuroblastoma cell lines and found that a majority express readily detectable levels of miR-380-5p, and cell lines with wild-type *TP53* generally had low expression of p53 protein (**Supplementary Fig. 4b**).

The *MYCN* gene is frequently amplified in human neuroblastomas, and overexpression of MYCN in transgenic mice directed by the tyrosine hydroxlase promoter (TH-*MYCN*) gives rise to neuroblastomas that recapitulate many features of the human disease[36]. Despite p53 being functional in these neuroblastomas, p53-driven apoptosis is minimal. Treatment of tumor-bearing mice with chemotherapy causes induction of p53, apoptosis and complete tumor remission[37]. TH-*MYCN* transgenic mice are among the most widely used *in vivo* models of human neuroblastoma, having been used extensively as a preclinical model with a proven good record in therapeutic validation[37–41]. These tumors are diverse primary cancers that, unlike cell lines, have not been through experimental clonal selection and years of *in vitro* culture. Notably, the mature miR-380-5p sequence and both miR-380-5p targets in the *p53* 3′ UTR are highly conserved between humans and mice. In the TH-*MYCN* transgenic neuroblastoma model, we found that miR-380-5p expression was on average five fold higher in primary tumors compared to benign sympathetic nervous tissue taken from either wild-type or *MYCN*-transgenic mice before the onset of disease (**Fig. 5a**).

We next examined miR-380-5p abundance in 205 primary human neuroblastoma samples collected from subjects before treatment with chemotherapy and compared it to human brain, the normal adult tissue with the highest expression of miR-380-5p (**Fig. 1b**). We found that miR-380-5p was readily detectable in 203 (99%) of 205 primary neuroblastomas (**Fig. 5b**) and substantially overexpressed, relative to normal brain, in 155 (76%) of 205 primary neuroblastoma samples (**Fig. 5b**). Expression of miR-380-5p did not correlate with individual age or tumor stage; however, tumors with *MYCN* amplification had significantly lower expression of miR-380-5p ($P < 0.001$). In these individuals, high miR-380-5p expression was associated with a significantly poorer outcome than in those with low expression of miR-380-5p (**Fig. 5c**; $P = 0.004$). In individuals without *MYCN*-amplified tumors, miR-380-5p expression was not associated with clinical outcome (**Supplementary Fig. 4c**). Furthermore, by analyzing miR-380 expression in both primary and secondary tumors, we conclude that miR-380-5p expression is maintained in distant metastases (**Supplementary Fig. 4d**). The finding that individuals whose tumors have both *MYCN* amplification and miR-380-5p overexpression have especially poor outcomes is consistent with data from various
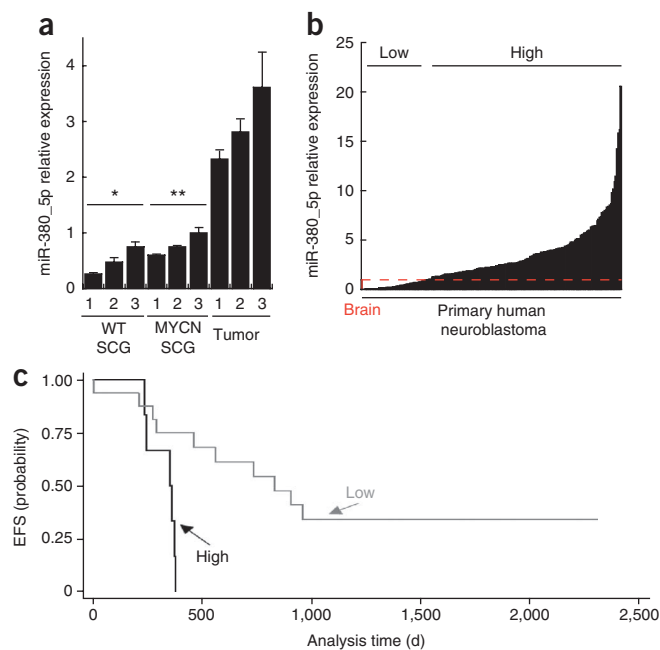
experimental model systems showing cooperation between MYC overexpression and attenuation of the p53 pathway in tumorigenesis.

miR-380-5p attenuates p53 function in neuroblastoma

The association of miR-380-5p expression with poor outcome in human neuroblastoma samples suggested a functional role in tumorigenesis. We transfected LNA-380 or two LNA controls into the *MYCN*-amplified NBL-WS human neuroblastoma cell line, which retains wild-type *TP53*, and examined cell proliferation and p53 expression. Inhibition of miR-380-5p resulted in a marked upregulation of p53 and p21[waf1] and PARP cleavage (**Fig. 6a** and **Supplementary Fig. 4e**). Diminished cellular viability after LNA-380 treatment was more pronounced than after treatment with the chemotherapeutic doxorubicin in these cells (**Fig. 6b,c**). Inhibition of miR-380-5p also resulted in p53 induction and impaired cellular proliferation in another *TP53*–wild-type human neuroblastoma cell line, SHEP (**Supplementary Fig. 4f,g**). In contrast, the BE(2)C line, taken from an individual at relapse and in which *TP53* has acquired an inactivating mutation[35], did not show any changes in cell viability in response to LNA-380 transfection (**Fig. 6a,c**). We conclude that miR-380-5p expression has a key role in suppressing wild-type p53 in human neuroblastoma.

miR-380-5p antagonist causes diminished tumor growth

We next examined whether miR-380-5p antagonists could alter the growth of neuroblastoma *in vivo* in a relevant orthotopic model. For this purpose, we chose a chimeric miRNA antagonist oligomer (anti-miR) that was modified at the 2′ position of the sugar with either a fluoro or a methoxyethyl group and a full phosphorothioate backbone. This design has been shown to produce potent inhibition of miRNAs *in vivo* (ref. 42 and E.G.M., unpublished observations). Primary tumors from transgenic TH-*MYCN* mice were orthotopically transplanted onto the kidney capsule of recipient BALB/c *nu/nu* mice. In this model, extensive neuroblastoma tumors form and envelop the kidney with a latency of approximately 3–5 weeks. Starting 2d after transplant, mice received systemic treatment via intraperitoneal injection of chimeric anti-miRs designed to antagonize miR-380
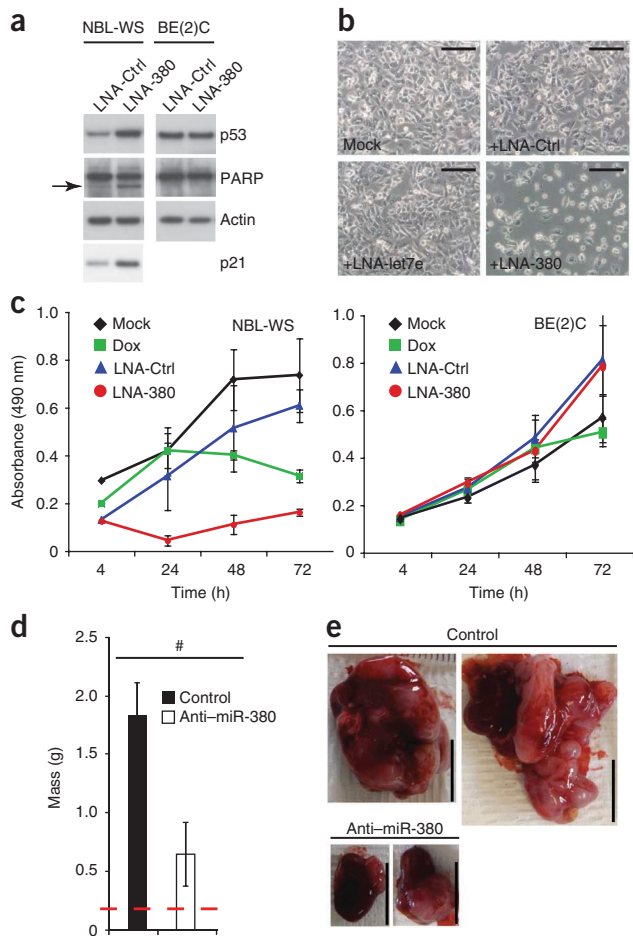
Figure 6 Treatment with miR-380-5p antagonist induces p53-dependent cell death in neuroblastoma cells and decreases tumor growth *in vivo*. (**a**) Western blots showing p53 and p21^{waf1} induction and PARP cleavage after knockdown of miR-380-5p by LNA-380 compared to control LNA in NBL-WS cells (left) but not *TP53*-mutant BE(2)C cells (right). Arrow indicates cleaved PARP. (**b**) Images of NBL-WS cells 24 h after mock transfection (mock) or treatment with the indicated LNAs; an LNA directed against let7e (LNA-let7e) was included as an additional control. Scale bars, 200 μm. (**c**) MTS (3-(4,5-dimethylthiazol-2-yl)-5-(3-carboxymethoxyphenyl)-2-(4-sulfophenyl)-2H-tetrazolium) assay showing that knockdown of miR-380-5p by LNA-380 induces rapid loss of cell viability in NBL-WS cells (left) but not BE(2)C cells (right). Dox, doxorubicin treatment. (**d**) Tumor size after systemic treatment with miR-380 antagonist (anti-miR380) for 3 weeks; mass depicted is the weight of the kidney (indicated by dashed red line) plus associated tumor (*n* = 5 mice for each treatment). (**e**) Representative images of kidneys and associated neuroblastoma tumor mass from two different mice for each treatment group. Scale bars, 1 cm. In **a**–**c**, results are representative of at least three independent experiments, error bars depict s.e.m. *$P < 0.01$.

(anti-miR380) or a control sequence twice weekly for 3 weeks (25 mg per kg body weight per injection). Treatment with anti-miR380 led to a markedly decreased size and weight of neuroblastoma tumors (**Fig. 6d,e**; $P = 0.01$). Anti-miR380–treated tumors also had diminished miR-380-5p and increased p21^{waf1} expression as compared to the control (**Supplementary Fig. 5a,b**). No toxicity was noted for mice treated with either anti-mir380 or control anti-miRs for 3 weeks (data not shown). We conclude that systemic delivery of a miR-380 antagonist diminishes the growth of orthotopically transplanted primary neuroblastoma tumors.

DISCUSSION

We have found that miR-380-5p is abundantly expressed in ES cells and provides a constitutive cell survival function by repressing expression of p53. We find that miR-380-5p antagonists act preferentially in ES cells that retain wild-type p53, indicating that p53 is a relevant target of miR-380-5p for this function. ES cells have an especially rapid rate of proliferation, lacking normal G1 and G2 phases, indicating that growth control pathways are attenuated. ES cells, however, retain an intact p53-MDM2-ARF tumor suppressor response that can be rapidly activated in times of cellular stress. Expression of miRNAs, such as miR-380-5p, may allow temporary and tunable repression of p53 in stem cells, thus permitting rapid cellular proliferation and self renewal, without the risks associated with irreversible loss of p53 function that is frequently found in cancer cells. Consistent with a dynamic role for miR-380-5p in regulating responses to cellular stress, we find rapid downregulation of this miRNA after ultraviolet treatment of ES cells, which correlates with upregulation of p53 expression.

Appropriate epigenetic imprinting of the locus encoding miR-380 has been recently shown to be crucial for the reprogramming of mouse fibroblasts into induced pluripotent stem (iPS) cells that are competent to give rise to a whole mouse[43]. The expression of transcripts from this region (as detected in ES cells) distinguishes iPS cells that will successfully contribute to chimeric mice from genetically identical iPS cells[43]. Repression of p53 expression promotes efficient iPS reprogramming[44], but whether expression of miR-380-5p or other miRNAs encoded from this locus are essential in the generation of iPS cells remains to be elucidated.

We have used neuroblastoma as a model disease in which to test the role of miRNA regulation of p53 in cancer. We show that nearly all neuroblastoma tumors express miR-380-5p and that high expression correlates with poor prognosis in individuals with *MYCN*-amplified disease. In human neuroblastoma cell lines, inhibition of miR-380-5p increases p53 expression and induces apoptotic cell death (**Supplementary Fig. 6**). Although p53 is the target we have studied most extensively, miR-380-5p is likely to target multiple mRNAs. We do not identify other miR-380-5p targets in this study, but we cannot exclude the possibility that miR-380-5p has other mRNA targets, some of which may also be involved in control of proliferation or survival.

A rapidly growing body of evidence has identified miRNAs as potential targets for cancer therapy. For example, overexpression of miR-26 by adeno-associated virus in a MYC-driven liver cancer model can attenuate tumor formation[45]. Likewise, a transgenic model that conditionally expresses miR-21 was used to show that tumor formation and maintenance was miRNA dependent, as tumor regression occurred after miR-21 expression was switched off[46]. The development of small miRNA antagonists has opened the possibility for the use of drug-like miRNA antagonists for cancer therapy. Inhibition of miR-10b by delivery of miRNA antagonists does not block primary tumor growth but can attenuate breast cancer metastasis in animal models[47]. Here we sought to determine whether miR-380 is required by tumors *in vivo* and found that treatment with anti–miR-380 results in diminished tumor growth. To our knowledge, this is the first report of decreased primary tumor growth in response to a systemically delivered *in vivo* treatment inhibiting a miRNA. We propose that miR-380 is an oncogene and a potential therapeutic target in p53 wild-type neuroblastoma. Specifically, whether inhibitors of miR-380-5p will sensitize tumors to genotoxic therapy is worth investigating in the clinic.

METHODS

Methods and any associated references are available in the online version of the paper at http://www.nature.com/naturemedicine/.

Note: Supplementary information is available on the Nature Medicine website.

1. Horn, H.F. & Vousden, K.H. Coping with stress: multiple ways to activate p53. *Oncogene* **26**, 1306–1316 (2007).
2. Levine, A.J., Hu, W. & Feng, Z. The P53 pathway: what questions remain to be explored? *Cell Death Differ.* **13**, 1027–1036 (2006).
3. Vogelstein, B. & Kinzler, K.W. Cancer genes and the pathways they control. *Nat. Med.* **10**, 789–799 (2004).
4. Petitjean, A., Achatz, M.I., Borresen-Dale, A.L., Hainaut, P. & Olivier, M. *TP53* mutations in human cancers: functional selection and impact on cancer prognosis and outcomes. *Oncogene* **26**, 2157–2165 (2007).
5. Vazquez, A., Bond, E.E., Levine, A.J. & Bond, G.L. The genetics of the p53 pathway, apoptosis and cancer therapy. *Nat. Rev. Drug Discov.* **7**, 979–987 (2008).
6. Martins, C.P., Brown-Swigart, L. & Evan, G.I. Modeling the therapeutic efficacy of p53 restoration in tumors. *Cell* **127**, 1323–1334 (2006).
7. Ventura, A. *et al.* Restoration of p53 function leads to tumour regression *in vivo*. *Nature* **445**, 661–665 (2007).
8. Xue, W. *et al.* Senescence and tumour clearance is triggered by p53 restoration in murine liver carcinomas. *Nature* **445**, 656–660 (2007).
9. Tweddle, D.A. *et al.* The p53 pathway and its inactivation in neuroblastoma. *Cancer Lett.* **197**, 93–98 (2003).
10. Yoon, H. *et al.* Gene expression profiling of isogenic cells with different TP53 gene dosage reveals numerous genes that are affected by *TP53* dosage and identifies CSPG2 as a direct target of p53. *Proc. Natl. Acad. Sci. USA* **99**, 15632–15637 (2002).
11. Zhao, R. *et al.* Analysis of p53-regulated gene expression patterns using oligonucleotide arrays. *Genes Dev.* **14**, 981–993 (2000).
12. Clarke, A.R., Gledhill, S., Hooper, M.L., Bird, C.C. & Wyllie, A.H. p53 dependence of early apoptotic and proliferative responses within the mouse intestinal epithelium following γ-irradiation. *Oncogene* **9**, 1767–1773 (1994).
13. Clarke, A.R. *et al.* Thymocyte apoptosis induced by p53-dependent and independent pathways. *Nature* **362**, 849–852 (1993).
14. Lowe, S.W., Schmitt, E.M., Smith, S.W., Osborne, B.A. & Jacks, T. p53 is required for radiation-induced apoptosis in mouse thymocytes. *Nature* **362**, 847–849 (1993).
15. Gottlieb, E. *et al.* Transgenic mouse model for studying the transcriptional activity of the p53 protein: age- and tissue-dependent changes in radiation-induced activation during embryogenesis. *EMBO J.* **16**, 1381–1390 (1997).
16. Venkatachalam, S. *et al.* Retention of wild-type p53 in tumors from p53 heterozygous mice: reduction of p53 dosage can promote cancer formation. *EMBO J.* **17**, 4657–4667 (1998).
17. Halaby, M.J. & Yang, D.Q. p53 translational control: a new facet of p53 regulation and its implication for tumorigenesis and cancer therapeutics. *Gene* **395**, 1–7 (2007).
18. Flynt, A.S. & Lai, E.C. Biological principles of microRNA-mediated regulation: shared themes amid diversity. *Nat. Rev. Genet.* **9**, 831–842 (2008).
19. Ventura, A. & Jacks, T. MicroRNAs and cancer: short RNAs go a long way. *Cell* **136**, 586–591 (2009).
20. Esquela-Kerscher, A. & Slack, F.J. Oncomirs—microRNAs with a role in cancer. *Nat. Rev. Cancer* **6**, 259–269 (2006).
21. Enright, A.J. *et al.* MicroRNA targets in *Drosophila*. *Genome Biol.* **5**, R1 (2003).
22. Saetrom, P. *et al.* Distance constraints between microRNA target sites dictate efficacy and cooperativity. *Nucleic Acids Res.* **35**, 2333–2342 (2007).
23. Zhao, Y., Samal, E. & Srivastava, D. Serum response factor regulates a muscle-specific microRNA that targets Hand2 during cardiogenesis. *Nature* **436**, 214–220 (2005).
24. Kuhn, D.E. *et al.* Experimental validation of miRNA targets. *Methods* **44**, 47–54 (2008).
25. Seitz, H. *et al.* A large imprinted microRNA gene cluster at the mouse Dlk1-Gtl2 domain. *Genome Res.* **14**, 1741–1748 (2004).
26. Tedeschi, A. & Di Giovanni, S. The non-apoptotic role of p53 in neuronal biology: enlightening the dark side of the moon. *EMBO Rep.* **10**, 576–583 (2009).
27. Le, M.T. *et al.* MicroRNA-125b is a novel negative regulator of p53. *Genes Dev.* **23**, 862–876 (2009).
28. Fu, L., Ma, W. & Benchimol, S. A translation repressor element resides in the 3′ untranslated region of human p53 mRNA. *Oncogene* **18**, 6419–6424 (1999).
29. Mazan-Mamczarz, K. *et al.* RNA-binding protein HuR enhances p53 translation in response to ultraviolet light irradiation. *Proc. Natl. Acad. Sci. USA* **100**, 8354–8359 (2003).
30. Sarkisian, C.J. *et al.* Dose-dependent oncogene-induced senescence *in vivo* and its evasion during mammary tumorigenesis. *Nat. Cell Biol.* **9**, 493–505 (2007).
31. Swarbrick, A., Roy, E., Allen, T. & Bishop, J.M. Id1 cooperates with oncogenic Ras to induce metastatic mammary carcinoma by subversion of the cellular senescence response. *Proc. Natl. Acad. Sci. USA* **105**, 5402–5407 (2008).
32. Welm, A.L., Kim, S., Welm, B.E. & Bishop, J.M. MET and MYC cooperate in mammary tumorigenesis. *Proc. Natl. Acad. Sci. USA* **102**, 4324–4329 (2005).
33. Hemann, M.T. *et al.* An epi-allelic series of p53 hypomorphs created by stable RNAi produces distinct tumor phenotypes *in vivo*. *Nat. Genet.* **33**, 396–400 (2003).
34. Scott, G.K. *et al.* Coordinate suppression of ERBB2 and ERBB3 by enforced expression of micro-RNA miR-125a or miR-125b. *J. Biol. Chem.* **282**, 1479–1486 (2007).
35. Tweddle, D.A., Malcolm, A.J., Bown, N., Pearson, A.D. & Lunec, J. Evidence for the development of p53 mutations after cytotoxic therapy in a neuroblastoma cell line. *Cancer Res.* **61**, 8–13 (2001).
36. Weiss, W.A., Aldape, K., Mohapatra, G., Feuerstein, B.G. & Bishop, J.M. Targeted expression of MYCN causes neuroblastoma in transgenic mice. *EMBO J.* **16**, 2985–2995 (1997).
37. Chesler, L. *et al.* Chemotherapy-induced apoptosis in a transgenic model of neuroblastoma proceeds through p53 induction. *Neoplasia* **10**, 1268–1274 (2008).
38. Liu, T. *et al.* Activation of tissue transglutaminase transcription by histone deacetylase inhibition as a therapeutic approach for Myc oncogenesis. *Proc. Natl. Acad. Sci. USA* **104**, 18682–18687 (2007).
39. Chesler, L. *et al.* Inhibition of phosphatidylinositol 3-kinase destabilizes Mycn protein and blocks malignant progression in neuroblastoma. *Cancer Res.* **66**, 8139–8146 (2006).
40. Hogarty, M.D. *et al.* ODC1 is a critical determinant of MYCN oncogenesis and a therapeutic target in neuroblastoma. *Cancer Res.* **68**, 9735–9745 (2008).
41. Rounbehler, R.J. *et al.* Targeting ornithine decarboxylase impairs development of *MYCN*-amplified neuroblastoma. *Cancer Res.* **69**, 547–553 (2009).
42. Davis, S. *et al.* Potent inhibition of microRNA *in vivo* without degradation. *Nucleic Acids Res.* **37**, 70–77 (2009).
43. Stadtfeld, M. *et al.* Aberrant silencing of imprinted genes on chromosome 12qF1 in mouse induced pluripotent stem cells. *Nature* **465**, 175–181 (2010).
44. Kawamura, T. *et al.* Linking the p53 tumour suppressor pathway to somatic cell reprogramming. *Nature* **460**, 1140–1144 (2009).
45. Kota, J. *et al.* Therapeutic microRNA delivery suppresses tumorigenesis in a murine liver cancer model. *Cell* **137**, 1005–1017 (2009).
46. Medina, P.P., Nolde, M. & Slack, F.J. OncomiR addiction in an *in vivo* model of microRNA-21–induced pre-B-cell lymphoma. *Nature* advance online publication, doi:10.1038/nature09284 (8 August 2010).
47. Ma, L. *et al.* Therapeutic silencing of miR-10b inhibits metastasis in a mouse mammary tumor model. *Nat. Biotechnol.* **28**, 341–347 (2010).

ONLINE METHODS

Bioinformatics. We determined local RNA structure as previously described[23] with mFold[48]. The *Homo sapiens* 3′ UTR average thermodynamic stability ($-\Delta G$) value of 16.2 ± 1.36 was calculated from the average of 30 3′ UTRs randomly selected from the Genbank database.

Orthotopic mammary transplant and tumorigenesis assays. We generated mice bearing mammary tumors by transplantation, essentially as previously described[32] with the following modifications. Mouse mammary epithelial cells were collected from female FVB/N mice (Jackson Laboratory) and virally transduced. We transplanted 500,000 cells into the cleared inguinal fat pads of naive 3- to 4-week-old female FVB/N mice. Mice were observed for tumor formation, tumor diameter was measured with calipers weekly and mice were killed at 42 d after transplant, or sooner if they had reached the ethical endpoint of the experiment. Animal experimentation was approved by the Committee for Animal Research at the University of California–San Francisco. Tumor tissue was either embedded in optimal cutting temperature medium or fixed in 4% paraformaldehyde, embedded in paraffin and processed for histology.

Transgenic mouse experiments. TH-*MYCN* transgenic mice (W. Weiss) develop neuroblastomas with a median of ~100 d[36]. We microdissected control SCG tissue from freshly killed wild-type 8- to 12-week-old 129S6 or control TH-*MYCN* mice; all non-nerve tissue was removed, and the tissue was snap frozen in liquid nitrogen. We prepared RNA from SCG or primary neuroblastoma tumors and performed qRT-PCR to determine miRNA expression.

Orthotopic neuroblastoma model and *in vivo* therapeutics. We transplanted primary neuroblastoma tumors from TH-*MYCN* transgenic mice (2 mm^3 per kidney capsule) into BALB/c *nu/nu* mice. Two days after transplant, mice were treated with chemically modified antisense oligonucleotides, designed to be complementary to miR-380-5p or a control anti-miR (Regulus Therapeutics). We treated mice twice weekly (25 mg per kg body weight per dose intraperitoneally) for 3 weeks and killed them a total of 4 weeks after transplant. The weight of the kidney plus the encompassing tumor or the contralateral kidney alone (not injected with tumor cells) was recorded. The median mass of the kidney alone was 0.17 g.

Clinical cohorts. Accrual and analysis of the Children's Oncology Group (COG) cohort was approved by the COG Neuroblastoma Subcommittee and the individual institutional review boards of all contributing institutions. The neuroblastoma clinical data set has been described elsewhere[49]. Accrual and analysis of the Children's Hospital Westmead cohort was approved by the Children's Hospital at Westmead Human Research Ethics Committee. Informed consent was obtained from parents or guardians of all subjects. All samples were de-identified, and researchers performing the miR-380-5p expression analysis were blinded to all clinical characteristics and the outcome of the subjects. We calculated event-free survival time from the time of enrollment on protocol 9047 of the COG cohort to the time of the first occurrence of an event (relapse, progressive disease, secondary malignancy or death), or to the date of last contact if no event occurred.

RNA expression analysis. We performed qRT-PCR assays (Taqman, Applied Biosystems) per the manufacturer's instructions with 25 ng (miRNA analysis) or 1 μg (*TP53*, *GAPDH*, *Gapdh* or *Cdkn1a*) total RNA prepared with RNABee (Iso-Tex Diagnostic), mirVana isolation kit (Ambion), Trizol (Invitrogen) or RNA was prepared previously for the COG protocol 9047 (ref. 49). We analyzed miR-380-5p expression in primary versus secondary disease by extracting RNA (Trizol) from snap-frozen tissue provided by the Children's Hospital Westmead Tumour Biobank. miR-380-5p expression was determined and expression was normalized to miR-16, small nuclear RNA *RNU6-2* and *RNU19* or small nucleolar RNA *sno202* levels, which are readily detectable endogenous controls and do not change much in the samples tested. We either isolated or purchased (Ambion, Stratagene) total RNA samples containing the small RNA fraction, followed by northern blot analysis for miR-380-5p or miR-380-3p as previously described[50].

Luciferase assays. For p53-3′ UTR reporters, the 104-bp conserved element from the human *TP53* 3′ UTR (WT p53) or a mutant lacking the mir-380-5p seed sequences (MUT p53) was cloned into a destabilized firefly luciferase vector (Promega) to generate reporter constructs. We transfected 293T cells with the indicated (**Fig. 3d**) miRNA expression vector, the reporter constructs and *Renilla* luciferase internal control vector and performed Dual-Glo reporter assays as indicated by the manufacturer (Promega).

For miR-380-5p perfect reporter, three consecutive binding sites with perfect complementarity to miR-380-5p were cloned into the pMIR-Report firefly luciferase vector (Ambion). We transfected NIH3T3 cells with 0.5 nM of the synthetic miRNA mimic (Ambion), the reporter constructs and *Renilla* luciferase internal control vector using Lipofectamine 2000 (Invitrogen). We transfected 50 nM LNA oligomers 24 h later and performed dual-Glo reporter assays after 48 h, following the manufacturer's instructions.

Statistical analyses. We computed cumulative event-free survival by the Kaplan-Meier method and compared between subgroups with the log-rank test. We tested the influence of selected factors on survival time with the Cox proportional hazards model. Specific factors considered as being possibly associated with outcome included *MYCN* amplification, age at diagnosis, neuroblastoma stage or miR-380-5p expression. We carried out statistical analyses with Stata, version 10.0 (StataCorp).

Additional methods. Details of plasmids, cell culture conditions, immunoblotting and immunohistochemistry can be found in the **Supplementary Methods**.

48. Zuker, M. Mfold web server for nucleic acid folding and hybridization prediction. *Nucleic Acids Res.* **31**, 3406–3415 (2003).
49. Haber, M. *et al.* Association of high-level MRP1 expression with poor clinical outcome in a large prospective study of primary neuroblastoma. *J. Clin. Oncol.* **24**, 1546–1553 (2006).
50. Grundhoff, A., Sullivan, C.S. & Ganem, D. A combined computational and microarray-based approach identifies novel microRNAs encoded by human gamma-herpesviruses. *RNA* **12**, 733–750 (2006).